A Technique for Analyzing Radiation from Conformal Antennas Mounted on Arbitrarily-Shaped Conducting Bodies

Dean Arakaki, Douglas H. Werner, and Raj Mittra
Department of Electrical Engineering
The Pennsylvania State University
University Park, PA 16802

1. ABSTRACT

This paper presents an efficient method to solve the problem of radiation from conformal aperture and microstrip antennas mounted on arbitrarily-shaped conducting bodies. The method, based on the surface equivalence and reciprocity principles, uses a combination of the Finite Difference Time Domain (FDTD) and Method of Moments (MoM) techniques to substantially improve the computational efficiency of the radiation pattern calculation. When the geometry and location of the radiating element are modified, only a small portion of the overall analysis requires re-simulation. This leads to a significant improvement in computational efficiency over presently-used techniques, and can substantially improve design efficiency when included in an optimization loop. The technique is first validated by solving two canonical problems, namely a thin slot which is oriented either axially or azimuthally on an infinitely long, perfectly conducting cylinder. These patterns are then compared to those produced by the same slots mounted on finite-length cylinders. Finally, patterns are computed for a cavity-backed elliptical patch antenna mounted on an infinite-length PEC cylinder and compared to patterns computed by an alternate method.

2. INTRODUCTION

Low profile conformal antennas for use on mobile communications systems are receiving widespread attention due to the advantages of minimized aerodynamic friction and radar cross-sectional area, reduced risk of antenna structural damage, and simplified construction requirements over conventional types. Since this type of antenna has a complex configuration and is usually mounted on a large structure, the simulation of these antennas continues to be a challenge. Methods that will accommodate complex structures such as FDTD and the Finite Element Method (FEM) require an excessive number of volume elements for large bodies. Surface methods such as the Method of Moments (MoM) that can model large structures are limited to relatively simple material compositions such as homogeneous or layered material structures. Thus, any of these methods used alone cannot efficiently model a typical conformal antenna; hence, the need for a combination of techniques.

Several combinations of simulation techniques have been used; the hybrid method used in this paper includes the MoM and FDTD. These methods were selected for their strengths in modeling large arbitrarily-shaped homogeneous conducting bodies and relatively small regions with a complex material structure, respectively. The link between the two methods is the reciprocity theorem, which relates the currents and fields between two systems [1-3].

The hybrid method used in this paper reduces computational requirements for the calculation of radiation patterns, especially when the shape of the radiating element and location on the mounting structure are modified. For most configurations, the size and shape of the mounting structure is fixed: the proposed method exploits this constraint by requiring analysis on this part of the problem only once. Instead of re-simulating the entire structure to obtain the aperture field distribution for every element shape and location change, this approach requires a re-simulation in the vicinity of the element only if the element shape is changed. The proposed hybrid method eliminates the need to carry out multiple computationally-intensive matrix operations encountered in the use of other simulation methods.

Since the FDTD technique is well-suited to the analysis of complex inhomogeneous structures, it is used to model the region which includes the cavity-backed conformal antenna and a sufficient volume around it to account for the effects of the surrounding environment on the radiating aperture field distribution. Through the surface equivalence principle, equivalent currents are found and the cavity region is closed with a perfect electrical conductor (PEC). The resulting structure, which can be large relative to the radiating aperture and of arbitrary shape, is analyzed by the MoM technique, since this method approximates the surface with triangular element discretization. This enhances both computational accuracy and efficiency via the use of a closely-fitting surface mesh of the PEC object, as opposed to using a volume discretization, which would be required in the FDTD method.

3. APPROACH

This paper utilizes the reciprocity principle to divide the original problem into two parts [1-3]. A reciprocity approach is also applied in [4]; however, the Finite Element Method (FEM) is used to compute the equivalent magnetic currents on surface S_1 instead of the Finite Difference Time Domain (FDTD) technique. First, we analyze the region containing the conformal antenna, which is typically inhomogeneous. The FDTD method is used for this analysis to derive equivalent electric and magnetic currents $\mathbf{J}$ and $\mathbf{M}$ on the surface S_1 (see Fig. 1) of the radiating aperture of the antenna. Next, S_1 is backed by a perfect electrical conductor (PEC) to short out the electric currents and the problem reduces to that of computing the radiation from these magnetic currents located on the *closed* PEC body. This calculation takes into account the shape of the PEC body in the vicinity of the antenna.

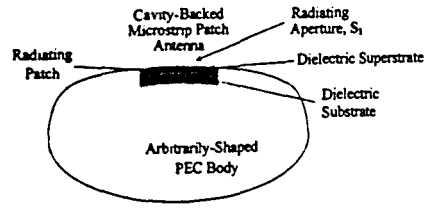

Fig. 1 Problem Geometry

The second step entails the application of the reciprocity principle to address the pattern computation problem. By invoking the reciprocity principle, we can write

$$\int_V \mathbf{E}_1 \cdot \mathbf{J}_2 \, dV = -\int_V \mathbf{H}_2 \cdot \mathbf{M}_1 \, dV \tag{1}$$

Our objective is to compute $\mathbf{E}_1$ radiated by $\mathbf{M}_1$ at a far-zone observation point P. We proceed by solving for the surface electric currents flowing on the closed PEC body by illuminating it with an infinitesimal dipole source $\mathbf{J}_2$ placed at location P. This problem is well-suited for handling by the Method of Moments (MoM). From the electric currents, the equivalent surface magnetic fields $\mathbf{H}_2$ are determined and by performing the integration on the right-hand side of (1), the desired field $\mathbf{E}_1$ is computed.

Note that once $\mathbf{H}_2$ is determined for the entire mounting structure, only $\mathbf{M}_1$ requires recalculation if the radiating element changes shape or location. The volume integral on the right-hand side of (1) reduces to the surface area of the superstrate (see Fig. 1). This re-simulation requires only a small percentage of the time required for a full-wave analysis of the entire mounting structure.

4. NUMERICAL RESULTS

To illustrate the procedure, we first compute the radiation pattern produced by a thin slot mounted on an infinite-length PEC cylinder. The slots are oriented in two directions: along the cylinder's axis (axial) and in the circumferential (azimuthal) direction. For the axial orientation, the aperture fields in the slot are ϕ-polarized (across the narrow width of the slot); thus, the $|E_\phi|$ pattern was computed. For the reciprocity calculation, the far-zone dipole source must be polarized in the same direction; therefore, analytical formulas taken from [5] to determine surface currents generated by a TE^z plane wave were used to obtain the necessary H fields (from the surface electric currents). For the azimuthal slot, the polarization of the aperture field is in the z-direction; thus, surface currents generated by a TM^z plane wave were used in the reciprocity pattern computation for $|E_\theta|$. The slot field variation was assumed to be cosinusoidal (dominant mode) and uniform along the length and width of the slot, respectively, for both orientations.

The reciprocity-approach patterns are compared to analytical formulations for these configurations [5] and are found to be in exact agreement (see Figs. 2 and 3 below).

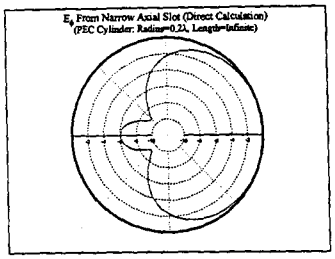

$|E_\phi|$ *vs.* ϕ Pattern (Direct) for Axial Slot in PEC Cylinder (Radius=0.2λ, Length=∞)

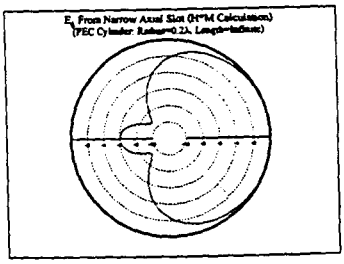

$|E_\phi|$ *vs.* ϕ Pattern (H*M) for Axial Slot in PEC Cylinder (Radius=0.2λ, Length=∞)

Fig. 2 Radiation Patterns: Axial Slot on Infinite-Length PEC Cylinder: Computation by Analytical (Direct) *vs.* Reciprocity (H*M) Methods

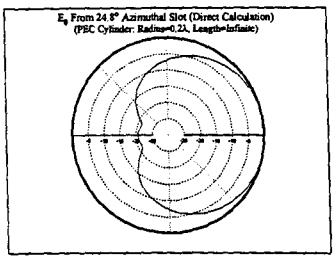

$|E_\theta|$ *vs.* ϕ Pattern (Direct) for Azimuthal Slot (24.8°) in PEC Cylinder (Radius=0.2λ, Length=∞)

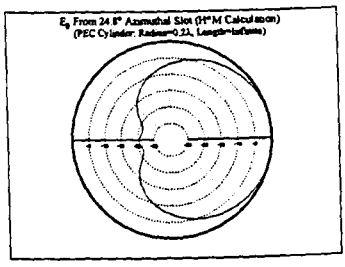

$|E_\theta|$ *vs.* ϕ Pattern (H*M) for Azimuthal Slot (24.8°) in PEC Cylinder (Radius=0.2λ, Length=∞)

Fig. 3 Radiation Patterns: Azimuthal Slot on Infinite-Length PEC Cylinder: Computation by Analytical (Direct) *vs.* Reciprocity (H*M) Methods

The above patterns are computed for slots mounted on a 0.2λ radius PEC cylinder. The subtended angle for the azimuthal slot is 24.8°, which is identical to the one in the example considered in [5].

Simulations were then carried out on finite-length cylinders. Since analytical formulas do not exist for surface currents generated by plane waves incident on finite-length cylinders, a numerical code (MoM) was used to obtain these currents. For the axial slot, the polarization of the slot aperture and therefore the far-zone dipole source are ϕ-directed. Hence, the truncation in the z-direction has a minimal effect on the pattern. This can be seen in the figure below which plots the patterns produced by axial slots mounted on 1λ, 2λ, and, infinite length PEC cylinders.

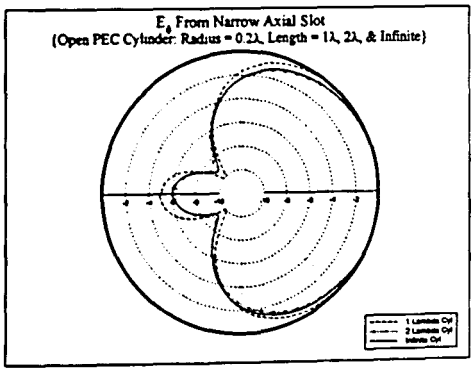

Fig. 4 $|E_\phi|$ vs. ϕ Radiation Patterns: Axial Slot on Finite-Length PEC Cylinders

The solid line represents the pattern for an axial slot mounted on an infinite cylinder. Thus, for a 2λ-length cylinder, the pattern has essentially converged to the infinite case. The pattern for the 1λ-length cylinder shows a higher back lobe level and deeper nulls caused by an enhanced standing wave presence created by the decreased distance to the truncated edge.

For the azimuthal slot, since the length of the cylinders had a significant impact on the shape of the patterns – an odd versus an even number of wavelengths – they are presented separately (see Fig. 5 below).

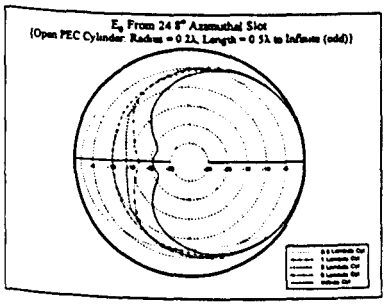

$|E_\theta|$ *vs.* ϕ: Odd λ-Length Cylinder

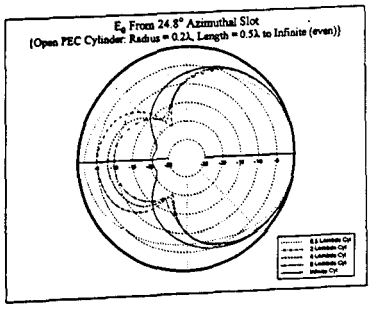

$|E_\theta|$ *vs.* ϕ: Even λ-Length Cylinder

Fig. 5 Radiation Patterns: Azimuthal Slot on Finite-Length PEC Cylinders

Again, the solid line shows the pattern produced by an azimuthal slot mounted on an infinite-length cylinder. The large back lobes for the even wavelength case are due to the current pattern formed on the finite cylinder when illuminated by a z-polarized plane wave. Since the truncation direction (z) is in the same direction as the

polarization of the plane wave, standing waves are formed with the number of peaks equaling the number of wavelengths. For the even wavelength case, the ϕ-cut at the z-midpoint passes through a local minimum in the current pattern on the lit (incident) side and a small local maximum on the shadow side of the cylinder. It is this shadow side peak that causes the large back lobe which appears in the patterns for the even case. For the odd case, the ϕ-cut at the z-midpoint passes through a local maximum on the lit side and a local minimum on the shadow side. This results in a smaller back lobe.

While the patterns appear to converge to the infinite case more closely for the odd wavelength case, both cases tend toward the infinite case as the length of the cylinder increases. The standing wave effects diminish only after the cylinder has reached a substantial length (beyond what could be simulated here), at which point both the odd and even wavelength cases begin converging to the infinite length case.

Finally, the radiation pattern produced by a cavity-backed elliptical patch antenna covered by a superstrate and mounted on an infinite-length PEC cylinder was computed. The radius of the cylinder is $0.631\lambda_o$ ($0.5\lambda_o + 0.2\lambda_d$). The patch considered for this analysis is elliptical with major and minor axes of $0.25\lambda_d$ and $0.2\lambda_d$, respectively, and was placed inside a rectangular block of dielectric ($\varepsilon_r = 2.33$) of length $1\lambda_d$ (x'-direction) and width $0.8\lambda_d$ (y'-direction) with a thickness of $0.2\lambda_d$. The major axis of the ellipse was aligned with the cylinder axis. A diagram of the conformal antenna is shown in Fig. 6 below.

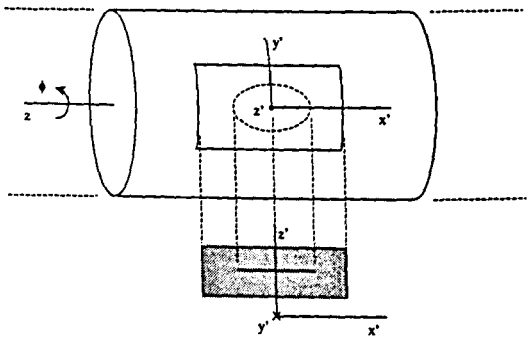

Fig. 6 Elliptical Patch Antenna Mounted on Infinite PEC Cylinder

The current distribution on the surface of the PEC cylinder is first calculated by analytical methods [5], followed by a computation of the electric fields (computed by a locally conformal FDTD code [6]) on the surface of the superstrate. The patch antenna is linearly polarized along the cylinder z-axis (patch x'-axis), hence the $|E_\theta|$ field ($\theta = 90°$) pattern is computed. This requires the computation of the surface electric currents produced on the cylinder by a z-polarized plane wave, which produces only z-directed currents. Therefore, only the x'-polarized aperture fields on the superstrate surface contribute to this pattern.

The resulting patterns were constructed by summing the complex dot-product of the electric current and electric field for each point on the surface of the superstrate and repeating this calculation while rotating the array of surface currents in the ϕ-direction. This dot-product is effectively the same as $\mathbf{H}_2 \cdot \mathbf{M}_1$ which appears on the right-hand side of (1), due to the normal vector being common to both vector quantities. The resulting pattern (H*M in Fig. 7 below) is compared to another obtained via the reciprocity theorem applied in a different manner. In this second approach, an infinite-length dielectric coated cylinder is considered, for which analytical formulas for the electric field inside the dielectric produced by an incident plane wave have been derived. The electric currents generated on the patch due to the feed (placed on the x'-axis halfway between the center and left edge) were computed using an MoM code. The MoM formulation assumes that the dielectric and backing ground plane are infinite in extent. These currents are then combined with the electric fields inside the dielectric at the location of the patch, and integrated over the surface of the patch to produce the radiation pattern. This plot is denoted E*J in the figure below.

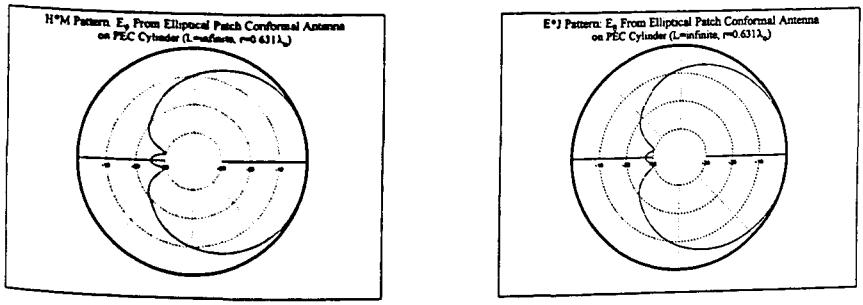

$|E_\theta|$ *vs.* ϕ: H*M Approach $|E_\theta|$ *vs.* ϕ: E*J Approach

Fig. 7 $|E_z|$ Radiation Patterns: H*M *vs.* E*J Reciprocity Approach

The two patterns are seen to compare well. The H*M approach pattern has a slightly higher back lobe level, most likely due to the truncation of the radiating aperture area. If the aperture area is increased, the relative energy transmitted in the forward direction will increase resulting in a reduced back lobe. Since the patterns compare well, the selected aperture size is considered sufficient.

5. CONCLUSIONS

This paper has presented an efficient method for determining radiation patterns for arbitrarily-shaped conformal antennas. Several examples were presented illustrating the procedure for computing a pattern using the reciprocity approach. The technique was first verified against known radiation patterns, then extended to more complex structures. The pattern produced by a cavity-backed elliptical patch antenna was also computed

and compared to a pattern constructed using an alternate method. The patterns were shown to be in good agreement.

The paper shows how results obtained for the mounting structure can be used for any radiating element shape and location on the structure in the computation of the radiation pattern. This feature of the technique results in significant improvements in computational efficiency when the shape or location of the radiating element is varied. Further work is being pursued on curved radiating patches using an extension of the present locally-conformal FDTD algorithm for the magnetic current calculation. The effect of curvature on the flat patch approximation to pattern computation will be addressed and quantified in terms of finding the limit when the approximation is no longer accurate.

REFERENCES

[1] R. Mittra, S. Dey, S. Chakravarty, and N. V. Veremey, "Reciprocity Approach to Pattern Computation of a Microstrip Antenna Operating in a Complex Environment," *IEEE AP-S International Symposium*, Atlanta, GA., 1998, pp. 1138-1141.

[2] D. H. Werner, G. D. Mouyis, and R. Mittra, "A Reciprocity Approach for Determining Radiation Patterns of Patch Antennas on Circularly-Cylindrical Platforms," *IEEE AP-S International Symposium*, Atlanta, GA., 1998, pp. 1582-1585.

[3] D. H. Werner, G. D. Mouyis, R. Mittra, and J. S. Zmyslo, "A Reciprocity Approach for Calculating Radiation Patterns of Arbitrarily Shaped Patch Antennas Mounted on Circularly-Cylindrical Platforms," *Proceedings of the 15th Annual Review of Progress in Applied Computational Electromagnetics (ACES)*, Naval Postgraduate School, Monterey, CA., March 15-20, 1999, pp. 508-515.

[4] J. M. Jin, J. A. Berrie, R. Kipp, and S. W. Lee, "Calculation of Radiation Patterns of Microstrip Antennas on Cylindrical Bodies of Arbitrary Cross Section," *IEEE Trans. Antennas Propagat.*, vol. 45, no. 1, pp. 126-132, Jan. 1997.

[5] R. F. Harrington, *Time-Harmonic Electromagnetic Fields*, McGraw-Hill, New York: 1961.

[6] S. Dey, R. Mittra, and S. Chebolu, "A Technique for Implementing the FDTD Algorithm on a Nonorthogonal Grid," *Microwave and Optical Technology Letters*, vol. 14, no. 4, March 1997.